



Observations and proxies of the surface layer throughflow in Lombok Strait

R. Dwi Susanto,¹ Arnold L. Gordon,¹ and Janet Sprintall²

Received 30 June 2006; revised 5 January 2007; accepted 31 January 2007; published 31 March 2007.

[1] Seasonal to interannual variability of the Lombok Strait surface layer transport is investigated. The geostrophic transport within the surface layer is estimated from the cross-channel pressure gradient measured by a pair of shallow pressure gauges positioned on opposing sides of Lombok Strait during 1996–1999. The Ekman transport through Lombok Strait, derived from scatterometer winds, is less than 10% or ~ 0.15 Sv of the estimated surface layer geostrophic transport. Monsoonal forcing is clearly evident in the regional sea surface height anomalies (SSHA) as derived from the satellite altimeter measurements. During the southeast monsoon, relatively low sea level is observed to the south of Lombok Strait, with relatively high sea level to the north; conditions reverse during the northwest monsoon. Estimated transports from the cross-channel pressure gradient, winds, SSHA and thermocline depth anomalies all reveal interannual variability associated with ENSO. Both the thermocline depth anomaly and the SSHA to the south of the East Java coast correlate significantly ($r = 0.7$) with the Lombok Strait total surface layer throughflow. The difference of SSHA from the south of the East Java coast minus the SSHA north of Lombok shows a higher correlation ($r = 0.84$). These high correlation values suggest that SSHA and thermocline depth anomalies can be used as proxies for the Lombok Strait surface layer throughflow. Qualitatively, such proxy transports agree with the surface transport inferred from the pressure gauges and Ekman transport in Lombok Strait from 1996 to 1999, and also with direct velocity measurements from current meter data obtained in 1985 and 2004–2005.

Citation: Susanto, R. D., A. L. Gordon, and J. Sprintall (2007), Observations and proxies of the surface layer throughflow in Lombok Strait, *J. Geophys. Res.*, 112, C03S92, doi:10.1029/2006JC003790.

1. Introduction

[2] As the only low-latitude interocean passage from Pacific to Indian Ocean, the Indonesian throughflow (ITF) plays an integral role in the global thermohaline circulation and directly impacts the basin mass, heat and freshwater budgets of these two large oceans [e.g., Bryden and Imawaki, 2001; Wijffels, 2001; Wajsowicz and Schneider, 2001; Gordon, 2001] with possible bearing on the El Niño Southern Oscillation (ENSO) and Asian-Australian (AA) monsoon climate phenomena [Webster *et al.*, 1998]. Lombok Strait is one of three major passages delivering the ITF into the Indian Ocean. While most of the ITF inflow channeled through Makassar Strait is advected to the Banda Sea before exported to the Indian Ocean within the Ombai and Timor passages, Lombok Strait provides a direct connection between the Makassar Strait and the Indian Ocean (Figure 1). Lombok Strait is located between the islands of Bali and Lombok, which is part of an east-west series of islands from Lombok to Timor that is collectively known as

Nusa Tenggara (Figure 1). Nusa Tenggara is strongly affected by the Asian-Australian monsoon system that is characterized by six-month reversals in the winds associated with the southeast and northwest monsoon. The peak of the southeast monsoon is in June–July–August while the northwest monsoon peak is in December–January–February.

[3] The first Lombok Strait throughflow in situ measurement was made during the Lombok Strait Experiment (LSE) in 1985–1986 [Murray and Arief, 1988] and more recently by the International Nusantara Stratification and Transport (INSTANT) program that began in December 2003 [Sprintall *et al.*, 2004]. Murray and Arief [1988] reported that the mean annual transport in 1985 was -1.7 ± 1.2 Sv (southward) with a maximum transport of -4.0 Sv during the boreal summer of the southeast monsoon. Hence, Lombok transport accounts for 20–25% of the Makassar transport [Susanto and Gordon, 2005], while the upper 100 m carries 50% of the total transport through Lombok Strait [Murray and Arief, 1988]. From December 1995 to April 1999 Lombok Strait transport of the upper 100 m has been inferred from a shallow pressure gauge array (SPGA [Chong *et al.*, 2000; Hautala *et al.*, 2001; Potemra *et al.*, 2002, 2003]). The inferred surface geostrophic transport through Lombok Strait showed strong variability over intra-seasonal to interannual timescales. Of particular interest, Hautala *et al.* [2001] showed strong northward geostrophic

¹Lamont-Doherty Earth Observatory of Columbia University, Palisades, New York, USA.

²Scripps Institution of Oceanography, La Jolla, California, USA.

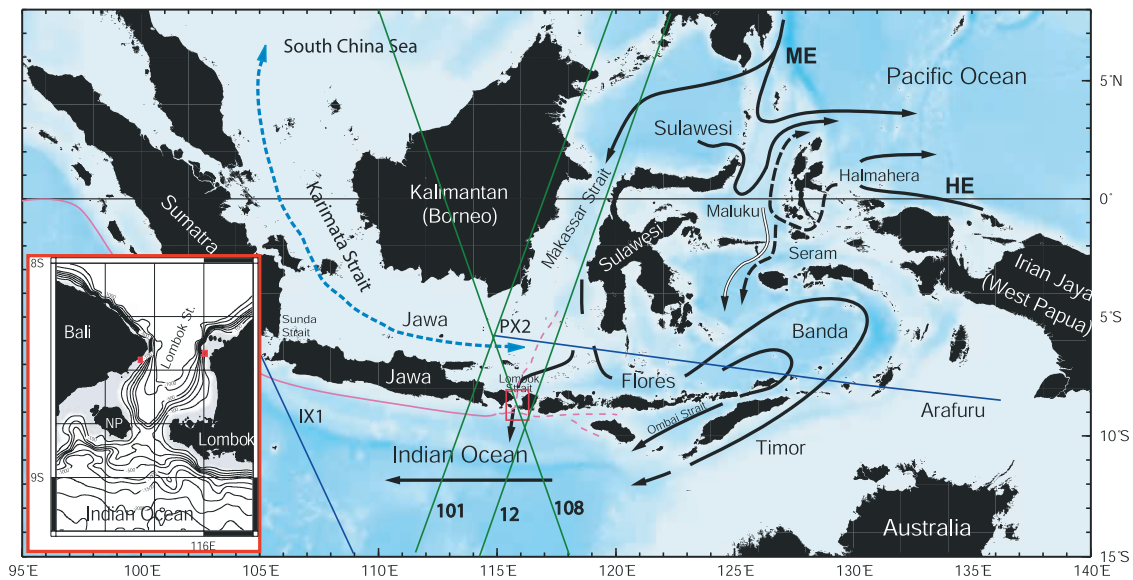


Figure 1. Map of Indonesian throughflow pathways from the Pacific Ocean to the Indian Ocean. The main throughflow pathway is Makassar Strait (west of Sulawesi) with an additional route to the east of Sulawesi. The main exit passages are through the Lombok and Ombai Straits and Timor Passage. Solid blue lines are IX1 and PX2 repeat XBT lines. Solid green lines represent two ascending tracks (#101 and #12) and one descending track (#108) of the TOPEX/Poseidon altimeter in the vicinity of the Lombok Strait. Solid magenta line is the path of a coastally trapped Kelvin wave from the equatorial Indian Ocean. The positions of a pair of shallow pressure gauges in the Lombok Strait are shown by the red squares (inset).

surface transport through Lombok Strait during the northwest monsoon coinciding with the 1998 La Niña, whereas many authors had previously suggested that the overall ITF into the Indian Ocean should increase during La Niña [e.g., Meyers, 1996; Fieux *et al.*, 1996; Field *et al.*, 2000; Susanto and Gordon, 2005]. This apparent contradiction suggests that either the main ITF entered the Indian Ocean through Lombok Strait at depth (and so was not measured by the surface pressure gauge measurements), or alternatively, the ITF inflow from Makassar Strait turned eastward into the Flores and Banda Seas and entered into the Indian Ocean via the other export passages of Ombai Strait and Timor Passage during this period. While the main goal of this paper is to fully describe the total surface layer variability within Lombok Strait, we will also discuss the potential likelihood of either or both of these hypotheses in serving to resolve this outstanding issue.

[4] Finally, there have been very few studies of the direct wind-driven Ekman contribution to the surface ITF transport and its variability. Arief [1992] observed an inconsistent relationship between the east-west wind and the north-south current through Lombok Strait during the LSE of 1985–86. In a recent study, Sprintall and Liu [2005] estimated the Ekman mass and heat transport across the Java and Flores Seas using the SeaWinds scatterometer wind fields from July 1999 to March 2005. They concluded that on monsoonal timescales, the wind driven Ekman flow could contribute significantly to the total volume and heat transport of the ITF through the exit passages, although their analysis did not directly resolve the Ekman transport through the individual passages. In this analysis, we will use scatterometer winds

derived from various satellites to directly determine the role of the regional monsoon wind in governing the surface throughflow variability in Lombok Strait from 1992 through 2005.

[5] The main aim of this paper is to comprehensively describe the seasonal to interannual variability of the surface layer ITF as it exits into the Indian Ocean through Lombok Strait. Our specific objectives are to: (1) determine the total surface layer (0–100 m) transport within Lombok Strait by combining the geostrophic transport calculated from the 1996–1999 shallow pressure gauge array data with the Ekman transport derived from regional wind as measured by satellite scatterometers; and (2) explore the possible link of regional thermal stratification and sea surface height anomaly (SSHA) to the total Lombok Strait surface layer throughflow, as estimated from the SPGA and wind data, for use as potential transport proxies on intraseasonal and longer timescales. The development of proxy measurements of the ITF transport is advantageous, as long-term direct measurements of the ITF are at present an expensive alternative and their implementation remains logistically challenging.

[6] The paper is organized as follows. In section 2, Ekman transport is estimated from zonal wind stress and compared to the geostrophic transport estimated from the pressure gauges. The response of the sea level variability to the south and north of Lombok Strait to the Ekman dynamics driven by the monsoonal winds is described. Section 3 discusses the possibility of using the SSHA south of the East Java coast, the difference of SSHA from the south of East Java coast minus that north of the Lombok coast, and the vertical thermal structure to the south of Lombok Strait as proxies

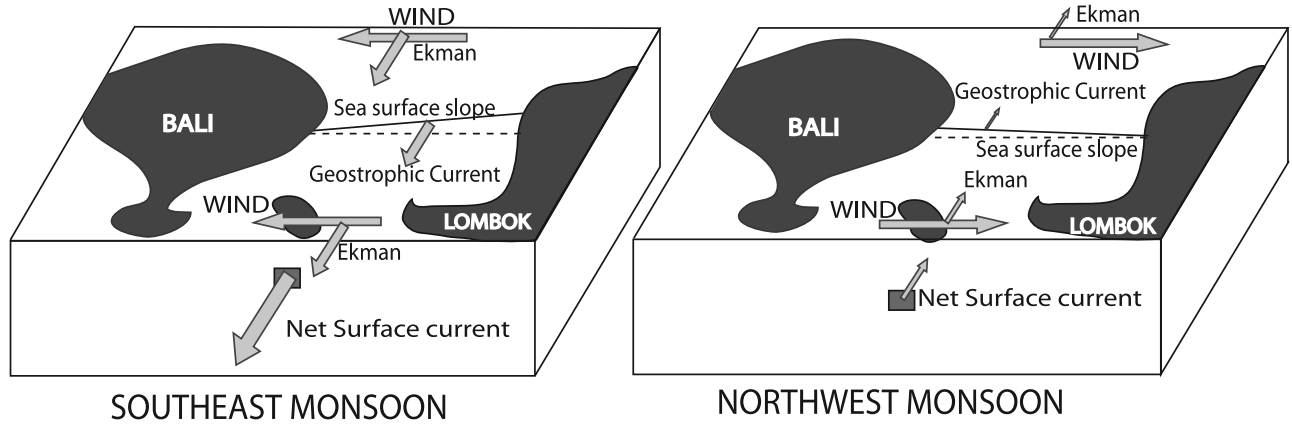


Figure 2. Schematic diagram of the surface flow within the Lombok Strait during the southeast monsoon (left) and northwest monsoon (right).

for the surface layer Lombok Strait throughflow. The conclusions are presented in section 4.

2. Throughflow Variability

2.1. Geostrophic Transport

[7] Along strait (meridional) flow through the Lombok Strait can be derived from the y -momentum equation. After applying a scaling argument with respect to Coriolis term, the y -momentum equation forms a balance between the Coriolis force, the pressure gradient and the friction terms associated with wind forcing [e.g., *Pond and Pickard*, 1983]. Assuming uniform zonal winds, the y -momentum balance can be written as:

$$fv = \frac{1}{\rho} \frac{\partial p}{\partial x} - K_z \frac{\partial \tau_{xz}}{\partial z} \quad \text{and} \quad \tau_{xz} = K_z \frac{\partial u}{\partial z} \quad (1)$$

where v is along-strait velocity; ρ is the density of the water ($\sim 1022.95 \text{ kg m}^{-3}$); p is the pressure which can be measured by the shallow pressure gauges on either side of Lombok Strait; x is the distance or width across the Lombok Strait (37 km); f is Coriolis $= 2\Omega \sin \Theta$ and is negative in the southern hemisphere, and Θ is latitude; τ_{xz} is zonal wind stress and K_z is vertical eddy viscosity.

[8] Rewriting the velocity term into two components associated with the geostrophic component and the Ekman velocity (ageostrophic) component, and neglecting the term $-A_z \frac{\partial^2 u_E}{\partial z^2}$ [because it is less than $10^{-3} (\frac{1}{\rho} \frac{\partial p}{\partial x})$], the total throughflow transport is the sum of the geostrophic transport and the Ekman transport. In the following analysis, we use the geostrophic flow and its transport (0–100 m depth) derived from the pair of pressure gauges deployed in Lombok Strait from December 1995 to April 1999. Since the vertical position of the gauges relative to the geoid is unknown, the pressure gauges only resolve the sea level fluctuations. However, *Hautala et al.* [2001] used the information from concurrent repeat ship-board ADCP surveys of 1–2 days duration across Lombok Strait to calibrate the sea level fluctuations, by scaling the inferred geostrophic surface flow to the tidally-corrected ADCP measured laterally-averaged velocity at 25 m depth. This yields the absolute shallow velocity and transport estimates, as used

by several previous investigators [*Chong et al.*, 2000; *Hautala et al.*, 2001; *Potemra et al.*, 2002, 2003]. The temporal sampling of the pressure gauge data is 1 hour. Since we are interested in the low frequency signal, a monthly low-passed filter has been applied to the geostrophic transport. A schematic diagram of the surface flow within the Lombok Strait (Figure 2) shows the expected response of the sea surface slope (and equivalently the pressure gradient) during the southeast monsoon (left) and northwest monsoon (right). The sign and strength of the geostrophic meridional velocity (v_g) is directly proportional to the pressure gradient dp/dx . For example, if the (pressure at Bali–pressure at Lombok) > 0 then $v > 0$, and the flow is to the north. In the following section, we use the estimate of geostrophic transport for the surface layer from the SPGA time series (as determined by *Hautala et al.* [2001]), and compare it to the Ekman transport estimated from satellite scatterometer winds.

2.2. Ekman Transport

[9] Following Ekman dynamics, during the northwest monsoon westerly (eastward) wind displaces water northward, causing a rise of sea level along the southern shores of the Nusa Tenggara island chain. North of Java and along the northern shore of Nusa Tenggara, sea level drops in response to this same monsoon wind field and presumably the Ekman transport and induced sea surface slope acts to reduce the Lombok surface throughflow. During the southeast monsoon, with easterly (westward) winds causing a rise of sea level along the northern shores of Java to Nusa Tenggara, the Ekman transport forces surface water southward and this is expected to enhance the Lombok surface throughflow into the Indian Ocean.

[10] High-resolution, along-track sea surface height data derived from TOPEX/Poseidon (T/P) cycles 1–354 and Jason-1 cycles 12–157, a total of 500 ten-day cycles spanning from September 1992 to April 2006, are used to show the sea level variability within the vicinity of Lombok Strait. The sea surface height anomaly (SSHA) data is the variability/anomaly of the sea surface height with respect to the Goddard Space Flight Center (GSFC00.1) Mean Sea State. This data set was provided by Brian Beckley (NASA-GSFC) and is based on an improved algorithm for process-

ing of the merged SSH data. In brief, the sea surface heights for T/P and Jason-1 (through Jason-1 cycle 127) are computed from the NASA GSFC replacement orbits that are based on the GGM02c gravity field within a consistent ITRF2000 terrestrial reference frame. In an effort to maintain consistency between T/P and Jason-1 SSHA, the GOT00.2 ocean tide model and the BM4 sea state bias correction based on the revised orbits is applied to both data sets. The decimeter level T/P and Jason-1 instrument bias has been removed. The last 30 cycles in the data set (Jason-1 cycles 128–157) are from the revised Jason-1 GDR_B. They are based on Eigen-04 orbits very similar to the GSFC orbits. The sea surface height has all the standard corrections applied including the revised MOG2D inverted barometer correction. For further details of the algorithm used for the SSHA data processing the reader is referred to *Beckley et al.* [2004].

[11] Within the vicinity of the Lombok Strait, the ascending track #101 passes the eastern tip of Java and track #12 passes the island of Lombok, and the descending track #108 passes through the Lombok Strait (solid green lines in Figure 1). From these tracks, an SSHA time series is computed from the average of the 25-s of the along track SSHA data before reaching or after passing a coastline. Thus, we use the 25-s averaged of SSHA along the ascending track #101, between latitudes 8.8529°S and 8.6572°S, which passes the eastern tip of south Java coast to represent the “south” SSHA. Similarly, the 25-s average of SSHA along the ascending track #12, between latitudes 8.1421°S and 7.9463°S, off the northern coast of Lombok is referred to as “north” SSHA. We also compared the along track SSHA time series to the weekly gridded SSHA obtained from the merged processing of T/P and European Remote Sensing Satellite (ERS-1/2) altimeter data from October 1992 to February 2002 within a similar region. To derive the gridded merged product of T/P and ERS-1/2 SSHA, standard corrections and some temporal and spatial interpolation techniques have been applied [*Le Provost, 2001; Le Traon et al., 1998*]. From 1992 to the end of 2001, the along track and merged gridded SSHA time series show a good agreement where merged data has a slightly smaller amplitude and is smoother compared to the along track data. However, starting in 2002, there is a discrepancy between these two data sets that is probably due to orbit bias error in the gridded SSHA product. Not only does the along track data provide a longer and higher resolution time series, but it also has been corrected for the orbit bias error [*Beckley et al., 2004*]. Therefore, we use the along track SSHA data to examine its possible link to the surface layer Lombok transport.

[12] The SSHA time series south and north of Lombok Strait, overlaid with the NIÑO3.4 index, are shown in Figure 3a. The monsoonal signal is clearly evident in sea surface height variability, particularly in the southern SSHA. During the northwest monsoon, the southern SSHA is higher than the northern SSHA; conditions are reversed during the southeast monsoon. Both the south and north SSHA have positive long-term averages that indicate the asymmetry of the monsoon strengths; stronger winds occur in the northwest monsoon than compared to the southeast monsoon. SSHA is more variable in the south compared to the north. This may be due to the larger expanse of open

water on the southern Indian Ocean side compared to the internal Indonesian Seas of the northern side, where the presence of more islands and shallower coastal regions may reduce the wind strength. Interannual variability is also apparent in the SSHA variability. As reported previously [e.g., *Susanto et al., 2000*], during the positive Indian Dipole in 1994 and the strong El Niño in 1997/1998 anomalous easterly winds act to enhance the upwelling strength and reduce the SSHA along the southern coasts of the Java-Nusa Tenggara islands. Conversely, the southern SSHA is higher during 1998/2000 La Niña than that during a normal year.

[13] Ekman transport sets up a difference in sea level between the northern and southern shores of Nusa Tenggara, which may be expected to introduce seasonal variability in the Lombok Strait throughflow. To estimate Ekman transport in the Lombok Strait, we use zonal wind stress from March 1991 to December 2004 derived from various scatterometer sensors (ERS-1/2, NSCAT and QuikSCAT) obtained from the CERSAT-IFREMER, France. The merged weekly ERS-1/2, NSCAT and QuikSCAT zonal wind stress north of the Lombok Strait is an average of the 112.5° to 117.5° E and 6.5° to 8° S region, and that south of the Lombok Strait is an average of the 112.5° to 117.5° E and 8.5° to 11.0° S region.

[14] Ekman transports both north and south of the Lombok Strait estimated from the wind stress data (Figure 3b), as expected are highly coherent at low frequencies, with strong seasonal variability due to the monsoons clearly evident. Southward flows are observed during the southeast monsoon and northward flows are observed during the northwest monsoon. This represents a modulation of the Lombok surface layer throughflow by the regional wind forcing. The apparent increase of the high frequency winds after July 1999 is probably due to higher resolution of the wind data: prior to this date the wind data are estimated from ERS-1/2 and NSCAT scatterometers, followed by an estimate from the higher resolution QuikSCAT scatterometer.

[15] According to *Barnett* [1983], the convergence of surface winds over the Indonesian region is subject to strong interannual variations in both its intensity and location. On interannual timescales, the Pacific trade winds are primarily influenced by ENSO. Here, we use the NIÑO3.4 index (Figure 3b) to indicate Pacific ENSO variability: positive NIÑO3.4 values correspond to El Niño periods, and negative values to La Niña. Reduced strength of the Ekman transport in Lombok Strait is associated with El Niño periods, notably that of 1997/98. Not only was the northward Ekman transport reduced during the northwest monsoon in 1997/98, but southward flows were also reduced during the southeast monsoon in 1997 and 1998 (Figure 3b).

[16] Variability of geostrophic velocity and the average Ekman transport north and south of the Lombok Strait is shown overlaid with the NIÑO3.4 index during the SPGA deployment period (Figure 3c). The SPGA deployment period coincided with both the 1997/98 El Niño event, and the La Niña event that began in mid-1998 and continued through to the end of 2000. In general the geostrophic flow and the Ekman transport are correlated, but during the La Niña period from mid-1998 there is an added northward

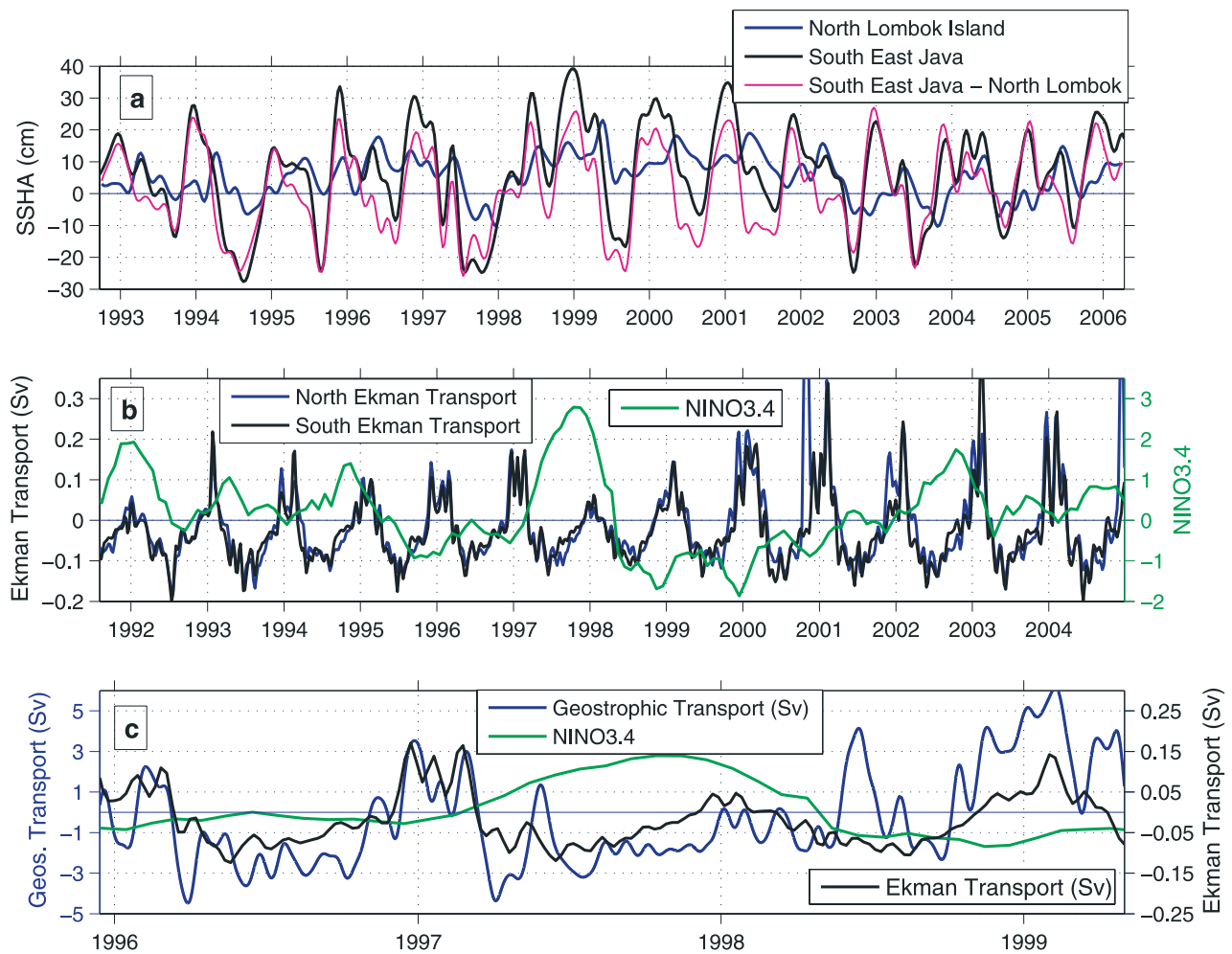


Figure 3. (a) Sea surface height anomaly (SSHA) in the southern coast of East Java (“south” SSHA) and northern coast of Lombok (“north” SSHA) and the differences between these two time series overlaid with NINO3.4 index. (b) Ekman volume transport (Sv) in the north and south of the Lombok Strait overlaid with NINO3.4 index. Seasonal reversal winds associated with Australian-Asian monsoon are dominant. Wind data derived from scatterometer sensors (ERS-1/2, NSCAT and QuikSCAT). Higher resolution wind data from QuikSCAT are available after July 1999. (c) Geostrophic current variability estimated from the pair of shallow pressure gauges and average Ekman transport in the north and south of the Lombok Strait overlaid with NINO3.4 index. Total transport is a sum of geostrophic and Ekman transports.

component of the Lombok Strait surface throughflow. The added northward component of the Lombok Strait surface throughflow during the northwest monsoon coinciding with the 1998 La Niña period is puzzling, as many authors have suggested that the overall ITF increases during La Niña [Meyers, 1996; Fieux et al., 1996; Ffield et al., 2000; Susanto and Gordon, 2005]. We will discuss this discrepancy in section 3.4. The correlation value between geostrophic velocity and average Ekman transport prior to May 1998 is 0.74. However, if we use the entire SPGA time series from December 1995 to April 1999, which includes the La Niña phase, the correlation value decreases to 0.6 although it is still significant at the 95% confidence level.

[17] The Ekman transport along all of Nusa Tenggara, on monsoonal timescales, could contribute significantly to the total volume of the ITF through the exit passages [Sprintall and Liu, 2005]. However, if we only consider the Lombok

Strait (a width of 37 km), the total Ekman transport is about 10% (~ 0.15 Sv, $1 \text{ Sv} = 10^6 \text{ m}^3/\text{s}$) of the geostrophic transport. Hence, in Lombok Strait, the total surface layer transport (Ekman + geostrophic) is dominated by the geostrophic component (Figure 3c).

3. Thermocline Depth and Sea Surface Height Anomalies as Throughflow Proxies

3.1. Thermal Stratification

[18] Following previous work by Ffield et al. [2000] who showed that there is correlation between thermocline depth and volume transport in the Makassar Strait at low frequencies (>3 month period), we investigate the relationship between thermocline depth anomaly in the regions north and south of the Lombok Strait to the total Lombok Strait surface layer volume transport (0–100 m). Thermocline

depth is represented by the depth of the midthermocline 22°C isotherm [Susanto *et al.*, 2000]. The thermal stratification at the northern entrance to Lombok Strait is determined from the repeat PX2 line along the northern Nusa Tenggara Islands (Figure 1), averaged within the box from 6.4°S to 7.0°S and 116.0°E to 117.5°E (referred to in the following as the northern box; Figure 4a). These XBT measurements are part of a continuing program [Wiffels and Meyers, 2004], maintained and quality controlled by the CSIRO-Australia (courtesy of Gary Meyers and Lidia Pigot).

[19] For the southern entrance to the Lombok Strait the nearest continuous XBT measurements are from the repeat IX-XBT line from Fremantle, Australia to the Sunda Strait (between Java and Sumatra Islands) which is about 1000 km west of the Lombok Strait (Figure 1). Hence, these data may not accurately represent the thermal structure immediately south of the Lombok Strait. In addition, there are only very few XBT/CTD data (~57 stations) available in this region from the NOAA-NODC and IFREMER, France databases from 1983–2002. Therefore, to represent thermal stratification in the southern entrance to the Lombok Strait, we use the SODA assimilation model output (<http://iridl.ldeo.columbia.edu/SOURCES/.CARTON-GIESE/.SODA/>). The SODA thermal data have a 0.5° longitude by 0.5° latitude spatial resolution, and we use the temperature data averaged within the box 9.75°S to 8.75°S and 115.25°E to 116.75°E (referred to as the southern box; Figure 4b). For the northern box, where both the in situ PX-2 XBT line and the SODA numerical data are available, the patterns of the thermal structure are found to be similar: the difference in thermocline depth varies from –27 m to 24 m, with zero mean and 10 m standard deviation for both time series. As we will show below, our conclusions remain the same using either the thermocline anomaly from the SODA data or the XBT data in the north of the Lombok Strait. This provides confidence that SODA can be used to accurately represent the thermal stratification at the southern entrance of Lombok Strait.

[20] Thermocline depth anomaly in the northern box varies from –25 m to 30 m relative to the long-term mean of 106 m (Figures 4a and 4b); while in the southern box the thermocline anomaly varies from –60 m to 40 m relative to the long-term mean of 94 m (Figures 4c and 4d). As indicated by previous investigators [e.g., Bray *et al.*, 1996; Susanto *et al.*, 2001; Field *et al.*, 2000], the thermocline depth anomalies are well correlated to the –NIÑO3.4 index, with the Indonesian seas thermocline being shallower during El Niño. For the thermocline depth anomaly in the northern box, the correlation to –NIÑO3.4 is 0.70 (Figure 4b), while in the southern box the correlation is 0.61 (Figure 4d). Figure 4e shows thermocline depth for the southern box derived from the SODA data minus the thermocline depth in the northern box derived using the PX2-XBT data (black line) and the SODA data (magenta line). During the El Niño and La Niña periods both the XBT and the SODA data show similar patterns and the same sign. In general both data sets show the thermocline depth in the southern box is shallower than the northern box, except during the strong La Niña in 1988 and in 1998–2000. During the strong El Niño events of 1986–87 and 1997–98, the thermocline depth in the southern box

was shallower by approximately 40 m than the thermocline depth in the northern box. This result is consistent with the positive SSHA difference shown between the southern coast of Java (south SSHA) and northern Lombok Strait (north SSHA) in Figure 3a during the 1998–2000 La Niña, when the Indian Ocean sea level south of the Lombok Strait is higher than that north of Lombok. Conditions are reversed during the El Niño events.

3.2. Throughflow Estimate Based on Southern Lombok Strait Thermocline Depth Anomaly

[21] To monitor ITF variability in the Indonesian region using in situ measurements is not only very expensive but also logistically challenging. Therefore, it is useful to generate a proxy record for the Lombok Strait throughflow. Over the Indian Ocean and Indonesian Seas, sea level and thermocline seasonal variations are negatively correlated (sea level rise corresponds to thermocline deepening) [Bray *et al.*, 1996]. Hence, this relationship suggests the potential for using the thermal stratification of the Lombok Strait region as a proxy for the surface layer throughflow. From the hydrostatic equation, the depth changes or heaving of the discontinuity are linearly related to the change of sea level:

$$\Delta h = \Delta Pz(\Delta\rho/\rho) \quad (2)$$

where Δh is the change in sea level associated with a change in pycnocline depth, ΔPz , relative to the long-term mean pycnocline depth. Average density in the surface layer ρ is 1022.95 kg m^{–3}, and the density difference $\Delta\rho$ between upper and lower layer is 3.27 kg m^{–3}. In the tropical regions, the pycnocline depth can be approximated by the thermocline depth from the 22°C isotherm [Susanto *et al.*, 2001].

[22] To investigate any possible link between the thermocline depth (at frequencies >3 months) and surface layer Lombok transport, we applied a three-month low-passed filter to the thermocline depth anomaly in the southern Lombok Strait derived from the SODA numerical model output as describe in section 3.1. Figure 5b shows the total surface layer Lombok transport from December 1995 to May 1999, thermocline depth anomaly in southern Lombok Strait from January 1980 to December 2001, and the –NIÑO3.4 index. Again, during the shallow pressure gauge deployment, there is a similar pattern between total Lombok transport and the thermocline depth anomaly. The correlation of the two time series is 0.7. Therefore, there is a possibility to use the thermocline depth anomaly as a proxy for the surface throughflow in Lombok Strait over periods longer than the intraseasonal timescale (3 months).

[23] To examine the link between thermocline depth anomaly and the total surface Lombok Strait throughflow, a linear regression analysis is applied and used to extrapolate the throughflow time series. Hence, we will have available a longer proxy of the throughflow time series since the thermocline depth anomaly data are available since 1980. The linear regression between the thermocline depth anomaly and Lombok transport time series is:

$$\begin{aligned} \text{Proxy Transport (Sv)} &= 0.06702 \\ &\times \text{thermocline depth anomaly (m)} - 0.3853 \end{aligned}$$

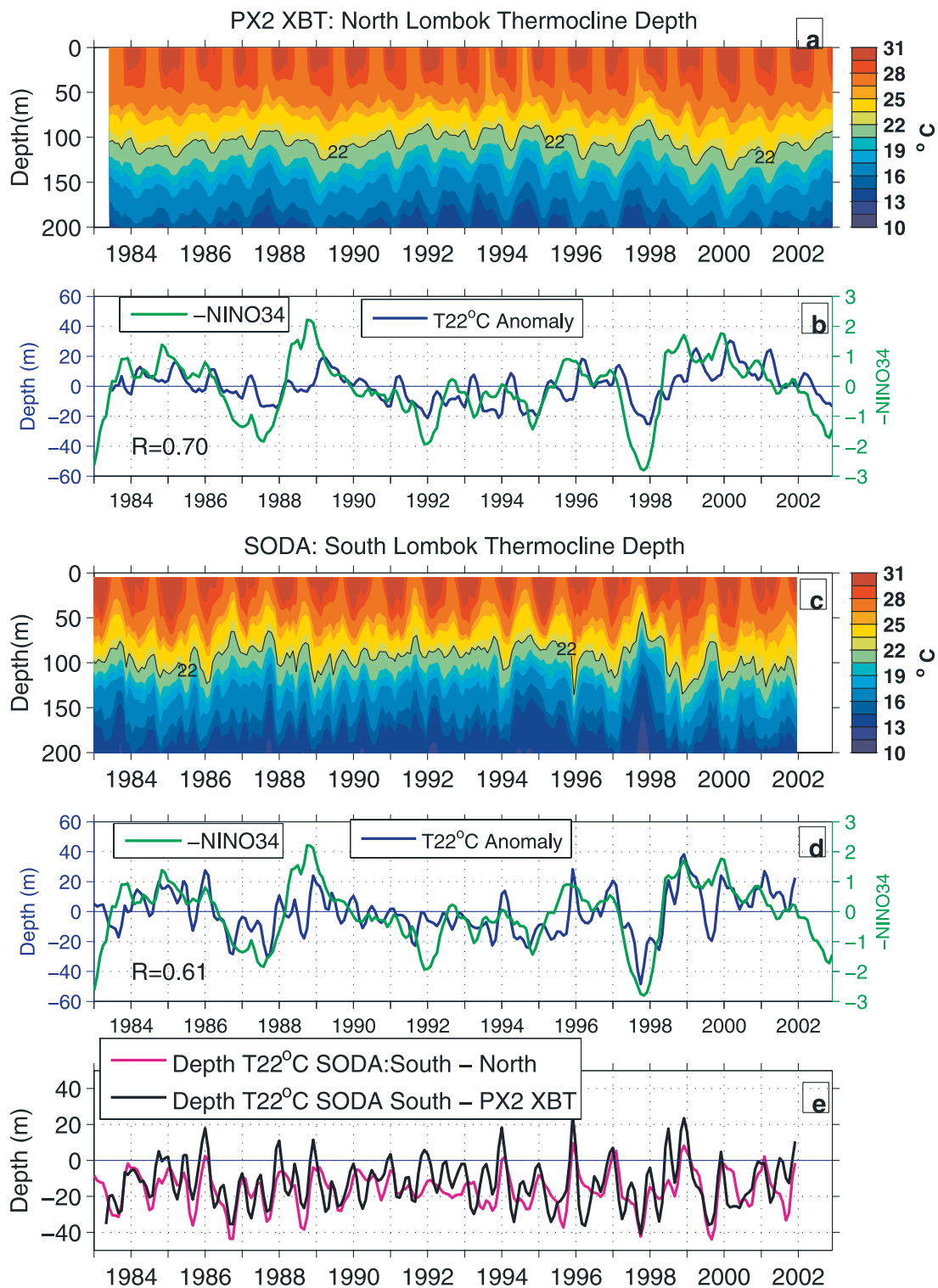


Figure 4. (a) Upper ocean thermal stratification in the Java/Flores Sea (north of the Lombok Strait) derived from the repeat PX2 XBT line (solid blue line in Figure 1). (b) Thermocline depth anomaly (long term mean has been removed) in the north of the Lombok Strait overlaid with the $-NINO3.4$ index. (c) Upper ocean thermal stratification south of Lombok Strait obtained from the SODA numerical model. (d) Thermocline depth anomaly (long-term mean has been removed) in the south of Lombok Strait overlaid with the $-NINO3.4$ index. (e) Difference of the thermocline depth to the south and north of Lombok Strait, based on both SODA data (magenta) and based on SODA in the south and XBT in the north (black).

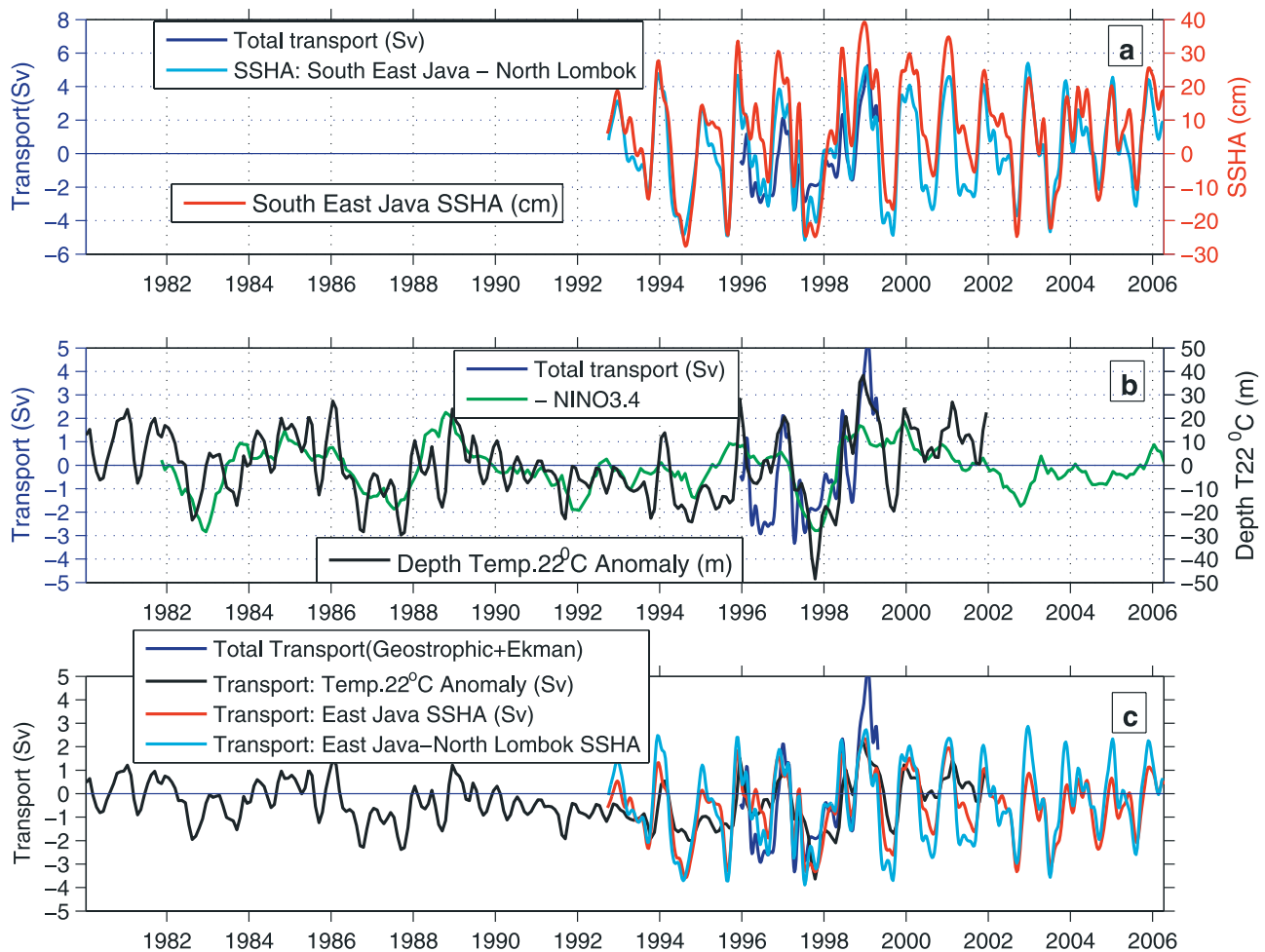


Figure 5. (a) Total Lombok Strait surface transport (dark blue line; negative sign toward the Indian Ocean), the sea surface height anomaly (SSHA) in the south of the East Java (red line) and the SSHA difference in the southern coast of East Java and northern coast of Lombok (light blue line). The correlation between the total transport and the south Java (south-north) SSHA is 0.7 (0.84). (b) Total surface transport in the Lombok Strait (dark blue line) and thermocline depth anomaly (depth of temperature at 22°C) obtained from the SODA numerical model in the south of the Lombok Strait (black line) overlaid with the $-\text{NINO}3.4$ index (green line). The correlation coefficient of the thermocline anomaly and $-\text{NINO}3.4$ is 0.7. The correlation between SSHA and thermocline depth anomaly from SODA numerical model in the south of the Lombok Strait is 0.8. (c) The total surface transport in Lombok Strait (dark blue line), and derived proxy estimates of the surface layer Lombok throughflow transport based on the thermocline depth anomaly (black line); SSHA to the south of Java (red line), and the (south of Java–north of Lombok) SSHA difference (light blue line).

The proxy transport based on the thermocline depth is shown in Figure 5c (solid black line) which spans from January 1980 to December 2001. The throughflow proxy based on the thermocline anomaly captures the seasonal variability of the transport signal very well. Based on this proxy, averaged over the 21 year time period the Lombok throughflow was southward with an average transport of -0.39 Sv and a standard deviation of 0.96 Sv.

3.3. Throughflow Estimate Based on Southern Java Sea Surface Height Anomaly (SSHA)

[24] A satellite sea level based index of ITF transport has been reported by *Potemra et al.* [1997] and *Potemra* [2005] using a combination of TOPEX/Poseidon sea level and

output from the Parallel Ocean Climate Model and Simple Ocean Data Assimilation-Parallel Ocean Program. Similarly, *Song* [2006] recently proposed a satellite based proxy of the large-scale ITF using the altimetric SSHA, a mean sea level field from GRACE, and Regional Ocean Model output. However, in both of these studies there was no estimate of the Lombok Strait transport because the studies were more concerned with the large-scale ITF, and moreover the models did not resolve the width of the Lombok Strait. We now explore the potential of using SSHA as a proxy for the surface layer Lombok Strait throughflow. To achieve this purpose, the along track SSHA (ascending track #101) passing the eastern tip of Java (referred as “south” SSHA time series described in section 2.2) is used.

Because it is an ascending track where the satellite passes northward from the open Indian Ocean before reaching the south Java coast, a high quality and complete time series of SSHA is expected. As with the thermocline depth anomaly time series, a three-month low-passed filter was applied to both the along track SSHA data and the total surface layer Lombok transport, as given by the addition of the geostrophic transport derived from the shallow pressure gauges and the Ekman transport derived from the scatterometer winds (e.g., Figure 3c). The southern SSHA time series from September 1992 to April 2006 and total Lombok Strait transport from December 1995 to May 1999 are shown in Figure 5a. Both time series show the same pattern for the 3.5-year overlap, and their correlation value is 0.7. This indicates that there is a link between SSHA south of Java and the surface layer Lombok Strait throughflow, and furthermore that SSHA in this region might also be used as a proxy for the throughflow transport. We also tried using the along track SSHA time series of descending and ascending tracks within the vicinity of the Lombok Strait (Figure 1): descending track #108 data (just north of Bali and inside the Lombok Strait and south of Lombok) and ascending track # 12 data (just south and north of Lombok). However, their correlations to the surface layer Lombok throughflow are lower ($r \sim 0.4$ to 0.6) than that of ascending data south of East Java. This suggests that Lombok Strait throughflow variability is strongly affected by the dynamics in the eastern Indian Ocean, that is by the Kelvin waves propagating along the southern coast of Sumatra and Java which are captured by the SSHA signal along the southern Java coast [Arief and Murray, 1996; Sprintall et al., 2000].

[25] As for the proxy based on the thermocline depth anomaly, we apply a linear regression analysis to the southern SSHA and the total surface Lombok transport time series. This regression value is used to extrapolate the throughflow time series from the beginning of T/P satellite altimeter in September 1992 to April 2006. The linear regression between the southern SSHA and Lombok transport time series is:

$$\text{Proxy Transport (Sv)} = 0.0887 \times \text{southern SSHA (cm)} - 1.1338$$

The proxy transport based on the southern SSHA is shown in Figure 5c (solid red line) which spans from September 1992 to April 2006. Similar to the proxy developed using the thermocline depth anomaly, the long-term mean of Lombok transport was southward with an average transport of -0.54 Sv over the 25-year time series, and a standard deviation of 1.31 Sv.

3.4. Throughflow Estimate Based on South–North Sea Surface Height Anomalies

[26] Many authors have suggested that the ITF increases during La Niña events [e.g., Meyers, 1996; Fieux et al., 1996; Field et al., 2000; Susanto and Gordon, 2005], but the pressure gauge data in the Lombok Strait shows an increase of northward surface throughflow during the northwest monsoon coinciding with the 1998 La Niña period. If the ITF is increased during La Niña, the northward surface

layer transport through Lombok Strait indicates that the La Niña enhanced ITF must exit the Indonesian seas to the east, within the passages on either side of Timor and/or be shifted to the subsurface throughflow within Lombok Strait. As discussed below, our data support the possibility of southward subsurface flow.

[27] One possible explanation for the northward Lombok Strait throughflow may be related to the regional distribution of surface layer buoyancy during La Niña relative to El Niño. During La Niña the surface water in the Lombok region is warmer and fresher [Sprintall et al., 2003]. In addition, the excess rainfall from the western Indonesian region is transported eastward from the Karimata Strait and Java Sea during the northwest monsoon, producing buoyant, low salinity surface water in the western Flores Sea between Makassar Strait and Lombok Strait. The buoyant freshwater induces a northward transport of the surface layer within Makassar Strait, counteracting southward winds and confines the main Makassar southward throughflow to the thermocline layer [Gordon et al., 2003; Susanto and Gordon, 2005]. Therefore, even though the ITF is expected to be relatively strong during La Niña, the buoyant and low salinity north of the Lombok Strait may inhibit the Makassar Strait surface throughflow from directly exiting into the Indian Ocean through the Lombok Strait. Thus, the Makassar throughflow can either be directly exported through the Lombok Strait beneath this buoyant-low salinity upper layer, and hence is not measured by the shallow pressure gauges in the Lombok Strait, or the Makassar thermocline throughflow turns eastward toward the Flores and Banda Sea due to the convergence in the Banda Sea during the northwest monsoon [Gordon and Susanto, 2001].

[28] Since the Ekman transport contribution to the total throughflow is very small, SSHA in the southern and northern coast of Nusa Tenggara are not only affected by the winds, but also by the vertical stratification associated with the density and temperature. As discussed in section 3.2 (equation (2)), there is a significant correlation between density stratification and sea surface height. Hence, SSHA to the south and north of Lombok Strait may be used to examine the possibility of subsurface flow in the Lombok Strait. The difference between SSHA in the southern tip of East Java (“south” SSHA) and north of Lombok (“north” SSHA) supports this hypothesis (Figure 3a). During the northwest monsoon coinciding with the La Niña period of 1998–2000, the SSHA south of Java is much higher than that north of Lombok (Figure 3a). Similar patterns were also observed during the weak 1995–1996 La Niña. During the 1994 Indian Ocean Dipole and the 1997/1998 El Niño events, the (south–north) SSHA difference is negative. Similarly, during the 1997/1998 El Niño event, the estimated geostrophic transport in the Lombok Strait is also negative (southward).

[29] The (south–north) SSHA difference overlaid with the total surface layer Lombok throughflow is shown in Figure 5a. Their correlation coefficient is 0.84, which is higher than if we use the south SSHA alone ($r = 0.7$) or thermocline depth anomaly ($r = 0.7$). This indicates that the sea surface height difference between south Java and north of the Lombok Strait can provide a better proxy for the Lombok throughflow. We again apply a linear regression

analysis to the (south-north) SSHA difference and the total surface Lombok transport time series:

$$\text{Proxy Transport (Sv)} = 0.1280 \times (\text{south} - \text{north}) \text{ SSHA (cm)} \\ - 0.5831$$

The proxy transport based on the (south-north) SSHA difference is shown in Figure 5c (solid cyan line), which spans the T/P satellite altimeter period from September 1992 to April 2006. Again, similar to the proxies developed using the south Java SSHA alone and the thermocline depth anomaly, using the (south-north) SSHA difference, the average Lombok transport is southward -0.43 Sv with a standard deviation much larger than the mean (1.65 Sv).

[30] We have examined the possibility of using the thermocline depth anomaly, SSHA in the south of Java, and the (south-north) SSHA difference as proxies for the surface Lombok transport (Figure 5c). All three time series show the same pattern and similar amplitudes. It is important to note that none of these three proxies show the anomalously strong northward flow during the northwest monsoon that coincided with the strong 1998/2000 La Niña as evident in the total transport derived from the pressure gauges and the wind-driven Ekman transport (Figure 5c). Hence, this means that they are probably doing a good job of getting the ITF transport right. That is, the proxies are capturing not just the surface flow (as shown by the pressure gauges and Ekman; Figure 3c) but also the southward flow at depth. Based on these proxies (thermocline depth, south SSHA, and south–north SSHA difference), for the last 25-years the average Lombok Strait throughflow was southward (~ -0.5 Sv) with variability ranges from 1–1.5 Sv. During the northwest monsoon the Lombok transport is northward, except during the northwest monsoons that coincide with the 1982/83, 1986/87, and 1997/98 El Niño events and the positive Indian Dipole events in 1994 and 1997, when the Lombok transport is southward.

[31] If we go back to the first measurement of the Lombok throughflow in 1985 [Murray and Arief, 1988], we find a qualitative agreement between the in situ flow measured by their current meter at 35 m depth (their Figure 3) and our predicted transport based on the thermocline depth anomaly (Figure 5c). Murray and Arief [1988] observed northward flows in February, April, and November–December 1985 and the rest of the year there was southward flow with maximum southward flow in August. These patterns are also seen in the predicted transport (Figure 5c). Based on the throughflow proxy using the southern Lombok Strait thermocline depth anomaly, the annual surface transport in 1985 was slightly northward 0.2 ± 0.7 Sv, which is in fairly good agreement with the Murray and Arief [1988] total volume transport (for the entire water column) of 1.7 ± 1.2 Sv southward.

[32] Based on a preliminary analysis of the upper 100 m along-strait velocity measurements from two INSTANT moorings in the Lombok Strait from January 2004 to July 2005 [Sprintall and Wijffels, 2006], there appears to be good qualitative agreement between the predicted surface layer transport based on the SSHA proxies that cover the same time period. Northward flows are observed in both east and west INSTANT moorings in the Lombok Strait in February–

March 2004, May 2004, December–March 2005, and June 2005. Similarly, during these periods, northward flows are also seen in the estimated transport based on both SSHA time series (Figure 5c). In the future, the final analysis of the three years from the INSTANT mooring data will be used to verify this predicted surface layer transport. Hence, at present, there appears to be a qualitative agreement between all the developed proxy transport estimates and the observed total surface layer transport in the Lombok Strait.

4. Conclusion

[33] The variability of the total surface layer transport of Lombok Strait is investigated by combining the geostrophic transport and the Ekman transport. The geostrophic transport is estimated from two shallow pressure gauges deployed on either side of the strait from December 1995 to May 1999 [Chong et al., 2000; Hautala et al., 2001]. The Ekman transport is estimated from the scatterometer winds from July 1991 to December 2004. The Ekman transport contribution to the total transport varies with the monsoon and ENSO, but the average contribution to the total transport is less than 10%.

[34] We have also explored the possible links of the total transport in Lombok Strait to the regional thermal stratification and SSHA variability. The SSHA, derived from newly available along-track altimeter data, varies with monsoon with relatively low sea level during the southeast monsoon along the southern coast of Nusa Tenggara and high sea level along the northern coast. The SSHA along the southern coast of East Java and thermocline depth anomaly vary with the total surface layer Lombok Strait throughflow, with the same correlation coefficients of $r = 0.7$. The SSHA difference between the south East Java coast minus the north Lombok coast has a higher correlation ($r = 0.84$) to the Lombok throughflow transport. Therefore, the SSHA south of Java coast, the (south–north) SSHA difference, and thermocline depth anomaly (as represented by the depth of the 22°C isotherm) can all be used as proxies for the throughflow using a linear regression analysis. All three proxies show similar patterns and none show any additional northward flow during the northwest monsoon coinciding with the 1998/2000 La Niña as shown by the geostrophic transport derived from the shallow pressure gauge data. This suggests that the transport proxies provide a suitable representation of the total ITF via Lombok Strait, that is, they resolve not only the surface flow but also the subsurface flow. In fact, recall that the absolute surface transport inferred from the shallow pressure data was obtained by referencing to the averaged ADCP velocity measured at 25 m depth [Hautala et al., 2001]. Our results suggest that if when the near-surface flow is northward then the main southward Throughflow occurs at depth, then a more appropriate reference level for the pressure fluctuations may be the velocity averaged over the top 100 m depth.

[35] The transport proxies developed in this analysis enable us to extend the estimated throughflow transport from January 1980 (based on the availability of thermal stratification) up to the present (our altimeter data end in April 2006). In the last quarter century, the average Lombok Strait throughflow is southward (~ -0.5 Sv) with a standard

deviation of $\sim 1\text{--}1.5$ Sv. The length of the proxy transport time series has also enabled us to examine the seasonal to interannual variability of the Lombok throughflow and its relationship to ENSO events. During the northwest monsoon coinciding with El Niño or positive Indian Dipole events, the Lombok Strait throughflow is southward (as opposed to the northward flow during the northeast monsoon typical of a normal year). The estimated throughflow qualitatively compares favorably with the observed 1985–1986 Lombok Strait throughflow [Murray and Arief, 1988] and to the first 1.5 years of the INSTANT program [Sprintall et al., 2004] time series. Thus, the development of proxies for throughflow transport are very important, not only because of the expenses and challenges associated with obtaining direct in situ measurements, but also because they enable us to explore the variability of the throughflow on timescales of relevance to long-term climate variability.

[36] **Acknowledgments.** This work was supported by the National Science Foundation [OCE-0219782 (D.S. and A.L.G.) and OCE-0220382 and OCE-0621601 (J.S.)] and by the Office of Naval Research grants N00014-04-1-0698 and N00014-05-1-0272 (D.S.). The authors gratefully acknowledge the useful comments and suggestions from the anonymous reviewers. Lamont-Doherty contribution 7003.

References

- Arief, D. (1992), Study on low frequency variability in current and sea-level in the Lombok Strait and adjacent region, Ph.D. dissertation, La. State Univ., Baton Rouge.
- Arief, D., and S. P. Murray (1996), Low-frequency fluctuations in the Indonesian throughflow through Lombok Strait, *J. Geophys. Res.*, *101*(C5), 12,455–12,464.
- Barnett, T. P. (1983), Interaction of the monsoon and Pacific trade-wind system at interannual time scales. 1, The equatorial zone, *Mon. Weather Rev.*, *111*(4), 756–773.
- Beckley, B. D., N. P. Zelensky, S. B. Lutcke, and P. S. Callahan (2004), Towards a seamless transition from TOPEX/Poseidon to Jason-1, *Mar. Geod.*, *27*, 273–389, doi:10.1080/01490410490889148.
- Bray, N. A., S. Hautala, J. Chong, and J. Pariwono (1996), Large-scale sea level, thermocline, and wind variations in the Indonesian throughflow region, *J. Geophys. Res.*, *101*(C5), 12,239–12,254.
- Bryden, H. L., and S. Imawaki (2001), Ocean transport of heat, in *Ocean Circulation and Climate*, edited by G. Siedler, J. Church, and J. Gould, Elsevier, New York.
- Chong, J. C., J. Sprintall, S. Hautala, W. L. Morawitz, N. A. Bray, and W. Pandoe (2000), Shallow throughflow variability in the outflow straits of Indonesia, *Geophys. Res. Lett.*, *27*(1), 125–128.
- Ffield, A., K. Vranes, A. L. Gordon, R. D. Susanto, and S. L. Garzoli (2000), Temperature variability within Makassar Strait, *Geophys. Res. Lett.*, *27*(2), 237–240.
- Fieux, M., C. Andrie, E. Charriaud, A. G. Ilahude, N. Metzl, R. Molcard, and J. C. Swallow (1996), Hydrological and chlorofluoromethane measurements of the Indonesian throughflow entering the Indian Ocean, *J. Geophys. Res.*, *101*(C5), 12,433–12,454.
- Gordon, A. L. (2001), Inter-ocean exchange, in *Ocean Circulation and Climate*, edited by G. Siedler, J. Church, and J. Gould, chap. 4.7, pp. 303–314, Elsevier, New York.
- Gordon, A. L., and R. D. Susanto (2001), Banda Sea surface layer divergence, *Ocean Dyn.*, *52*(1), 2–10.
- Gordon, A. L., R. D. Susanto, and K. Vranes (2003), Cool Indonesian throughflow as a consequence of restricted surface layer flow, *Nature*, *425*(6960), 824–828.
- Hautala, S. L., J. Sprintall, J. T. Potemra, J. C. Chong, W. Pandoe, N. Bray, and A. G. Ilahude (2001), Velocity structure and transport of the Indonesian Throughflow in the major straits restricting flow into the Indian Ocean, *J. Geophys. Res.*, *106*(C9), 19,527–19,546.
- Le Provost, C. (2001), Ocean tides, in *Satellite Altimetry and Earth Sciences, a Handbook of Techniques and Applications*, edited by L. L. Fu and A. Cazenave, 463 pp., Elsevier, New York.
- Le Traon, P. Y., F. Nadal, and N. Ducet (1998), An improved mapping method of multi-satellite altimeter data, *J. Atmos. Oceanic Technol.*, *25*, 522–534.
- Meyers, G. (1996), Variation of Indonesian throughflow and the El Niño Southern Oscillation, *J. Geophys. Res.*, *101*(C5), 12,255–12,263.
- Murray, S. P., and D. Arief (1988), Throughflow into the Indian Ocean through the Lombok Strait, January 1985–January 1986, *Nature*, *333*(6172), 444–447.
- Pond, S., and G. Pickard (1983), *Introductory Dynamical Oceanography*, 2nd ed., 329 pp., Elsevier, New York.
- Potemra, J. T. (2005), Indonesian throughflow transport variability estimated from satellite altimetry, *Oceanography*, *18*, 98–107.
- Potemra, J. T., R. Lukas, and G. Mitchum (1997), Large-scale estimation of transport from the Pacific to Indian Ocean, *J. Geophys. Res.*, *102*(C13), 27,795–27,812.
- Potemra, J. T., S. L. Hautala, J. Sprintall, and W. Pandoe (2002), Interaction between the Indonesian Seas and the Indian Ocean in observations and numerical models, *J. Phys. Oceanogr.*, *32*(6), 1838–1854.
- Potemra, J. T., S. L. Hautala, and J. Sprintall (2003), Vertical modes of the Indonesian Throughflow in a large scale model, *Deep Sea Res., Part II*, *50*, 2143–2162.
- Song, Y. T. (2006), Estimation of interbasin transport using ocean bottom pressure: Theory and model for Asian marginal seas, *J. Geophys. Res.*, *111*, C11S19, doi:10.1029/2005JC003189.
- Sprintall, J., and W. T. Liu (2005), Ekman mass and heat transport in the Indonesian Seas, *Oceanography*, *18*(4), 60–69.
- Sprintall, J., and S. Wijffels (2006), A first-look at variability in the Indonesian throughflow from the INSTANT moorings in Lombok and Ombai Straits, *Eos Trans. AGU*, *87*(36), Ocean Sci. Meet. Suppl., Abstract OS34C-04.
- Sprintall, J., A. L. Gordon, R. Murtugudde, and R. D. Susanto (2000), A semiannual Indian Ocean forced Kelvin wave observed in the Indonesian seas in May 1997, *J. Geophys. Res.*, *105*(C7), 17,217–17,230.
- Sprintall, J., J. T. Potemra, S. L. Hautala, N. A. Bray, and W. Pandoe (2003), Temperature and salinity variability in the exit passages of the Indonesian Throughflow, *Deep Sea Res.*, *50*, 2183–2204.
- Sprintall, J., S. Wijffels, A. L. Gordon, A. Ffield, R. Molcard, R. D. Susanto, I. Soesilo, J. Sopaheluwakan, Y. Surachman, and H. M. van Aken (2004), A new international array to measure the Indonesian Throughflow: INSTANT, *Eos Trans. AGU*, *85*(39), 369.
- Susanto, R. D., and A. L. Gordon (2005), Velocity and transport of the Makassar Strait throughflow, *J. Geophys. Res.*, *110*, C01005, doi:10.1029/2004JC002425.
- Susanto, R. D., A. L. Gordon, J. Sprintall, and B. Herunadi (2000), Intra-seasonal variability and tides in Makassar Strait, *Geophys. Res. Lett.*, *27*(10), 1499–1502.
- Susanto, R. D., A. L. Gordon, and Q. Zheng (2001), Upwelling along the coasts of Java and Sumatra and its relation to ENSO, *Geophys. Res. Lett.*, *28*(8), 1599–1602.
- Wajswowicz, R. C., and E. K. Schneider (2001), The Indonesian throughflow's effect on global climate determined from the COLA coupled climate system, *J. Clim.*, *14*, 3029–3042.
- Webster, P., V. Magana, T. Palmer, J. Shukla, R. Tomas, M. Yanai, and T. Yasunari (1998), Monsoons: Processes, predictability, and the prospects for prediction, *J. Geophys. Res.*, *103*, 14,451–14,510.
- Wijffels, S. E. (2001), Ocean transport of freshwater, in *Ocean Circulation and Climate*, edited by G. Siedler, J. Church, and J. Gould, Elsevier, New York.
- Wijffels, S. E., and G. Meyers (2004), An intersection of oceanic waveguides: Variability in the Indonesian throughflow region, *J. Phys. Oceanogr.*, *34*, 1232–1253.

A. L. Gordon and R. D. Susanto, Lamont-Doherty Earth Observatory of Columbia University, Palisades, NY 10964, USA. (dwi@ldeo.columbia.edu)

J. Sprintall, Scripps Institution of Oceanography, La Jolla, CA 92093, USA.